Electronic Supplementary Material (ESI) for Journal of Materials Chemistry A


*Electronic Supplementary Information*

# A new solid oxide molybdenum-air redox battery

Xuan Zhao, Yunhui Gong, Xue Li, Nansheng Xu and Kevin Huang*

Department of Mechanical Engineering, University of South Carolina, Columbia, SC

29201

## Phase diagram of Mo-O system

According to phase diagram of Mo-O system shown in Fig.S1, Mo-$MoO_2$ is considered as a chemically stable redox couple suitable for energy storage medium (ESM) within the temperature window of interest.

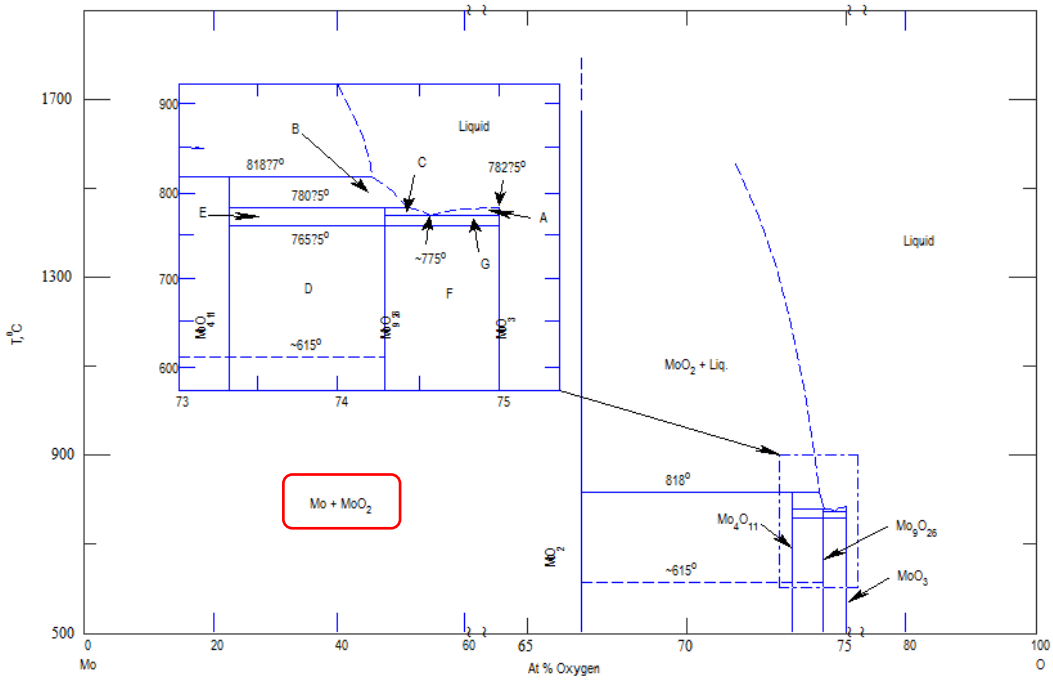


**Fig. S1.** Phase diagram of the Mo-O system [1]

## Calculation of $q_{max}$ and $J_{max}$

The premise for calculating $q_{max}$ and $J_{max}$ is that the rate of charge-transfer (current) of RSOFC must match to the rate of the redox reactions in order to sustain the battery's functionality. The deduction of $q_{max}$ and $J_{max}$ equations starts from the parabolic kinetics governing the redox reaction:

$$(\Delta m)^2 = K_p \cdot t \quad (1)$$

here $\Delta m$ is the mass change of the sample, g/cm$^2$; $K_p$ is the parabolic rate constant of redox kinetics, g$^2$/cm$^4$/sec; t is the time in seconds. Combing the global reaction shown in Fig.1 with Faraday's law yields the $q_{max}$ (Ah/g) of the battery:

$$q_{max} = \frac{\Delta m \cdot S_{ESM}}{3600 \cdot M_O} \cdot 2F \cdot x \quad (2)$$

where $M_O$ is the atomic weight of oxygen, 16g/mole; *x* is the oxygen stoichiometry of $MeO_x$; $S_{ESM}$ is the specific surface area of the redox materials in ESM, cm$^2$/g. Substituting eq. (1) into eq. (2) leads to $q_{max}$:

$$q_{max} = \frac{2F \cdot x \cdot \sqrt{K_p \cdot t}}{3600 \cdot M_O} \cdot S_{ESM} \quad (3)$$

The equivalent maximum current density, $J_{max}$ (A/cm$^2$), of RSOFC then equals

$$J_{max} = \frac{3600 \cdot q_{max}}{t \cdot A_{RSOFC}} \cdot m_{ESM} = \frac{2F \cdot x \cdot \sqrt{K_p / t}}{M_O \cdot A_{RSOFC}} \cdot (S_{ESM} \cdot m_{ESM}) \quad (4)$$

where $m_{ESM}$ and $A_{RSOFC}$ are the mass loading of the redox material in ESM and the active electrode area of RSOFC, respectively. $m_{ESM}$ and $A_{RSOFC}$ are set to 1 gram and 1 cm$^2$, respectively, while $S_{ESM}$ is taken as 1,000 cm$^2$/g for the case study.

Due to the scarcity of kinetic rate constants $K_P$ relevant to the metal-oxidation/ oxide-reduction in $H_2O$–$H_2$ mixture, we have used the $K_p$ values obtained from air oxidation in the calculation instead. [3-5] Since the rate of metal oxidation in the presence of steam could be faster than that in air because of faster surface reaction and more porous scale formed, the air-oxidation estimated $J_{max}$ may be conservative.

## Preparation of RSOFC

A $La_{0.8}Sr_{0.2}Ga_{0.83}Mg_{0.17}O_{3-\delta}$ [6] (LSGM) electrolyte-supported button cell with an effective electrode area of 1.3cm$^2$ was used as the RSOFC. The fuel electrode consisted of two layers of LDC ($Ce_{0.6}La_{0.4}O_{2-\delta}$)-Ni and GDC ($Ce_{0.8}Gd_{0.2}O_{2-\delta}$)-Ni was screen-printed from the respective pastes on one side of the LSGM surface, while the air-electrode was made by infiltrating a prefabricated porous LSGM-scaffold with a mixture of $Sm_{0.5}Sr_{0.5}CoO_{3-\delta}$ and $Sm_{0.2}Ce_{0.8}O_{1.9}$ (SSC/SDC) nitrate solutions for multiple times. [7] The structure of the RSOFC is illustrated in Fig.S2. The compositions and dimensions of the components in this RSOFC are summarized in Table S1.

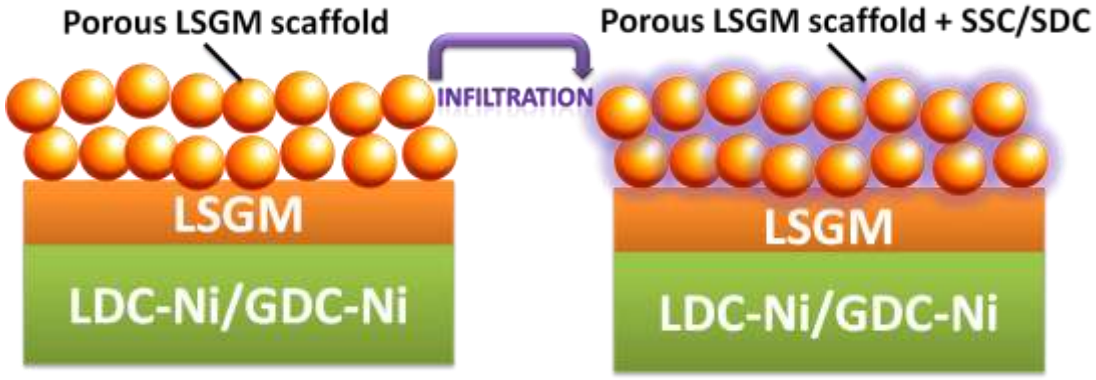


**Fig.S2.** Schematic of RSOFC applied in the battery test

**Table S1 Materials employed in RSOFC of the Mo-air redox battery**

| Component | Composition | Thickness (μm) |
|---|---|---|
| **Fuel electrode** | LDC-Ni/GDC-Ni | 30 |
| **Electrolyte** | LSGM | 350 |
| **Air electrode** | Porous LSGM-SSC/SDC | 100 |
| **Current collector** | Silver paste/platinum mesh | 10 |

## Characterizations

Fig.S3 shows the cross-section of the post-tested RSOFC, including all three functional layers. The contacts between electrolyte and electrodes are well maintained, showing no delamination occurred during the battery test, see Fig.S3 (a). Fig.S3 (b) shows that the infiltrated SSC/SDC particles remain finely dispersed in the porous LSGM after test, while Fig.S3(c) also indicates a porous structure after test.

Fig.S4 shows the fuel cell performance of RSOFC measured from 650$^{o}$C to 550$^{o}$C in an open system with a flowing $H_2$+3%$H_2O$ as the fuel. The maximum power density of the RSOFC is only 32mW/cm$^2$ and area specific resistance (ASR) is 26 Ωcm$^2$ at 550$^{o}$C, respectively. This low RSOFC performance severely limits the overall performance of the battery. One recent effort in our lab is to further improve the low-temperature performance of RSOFC.

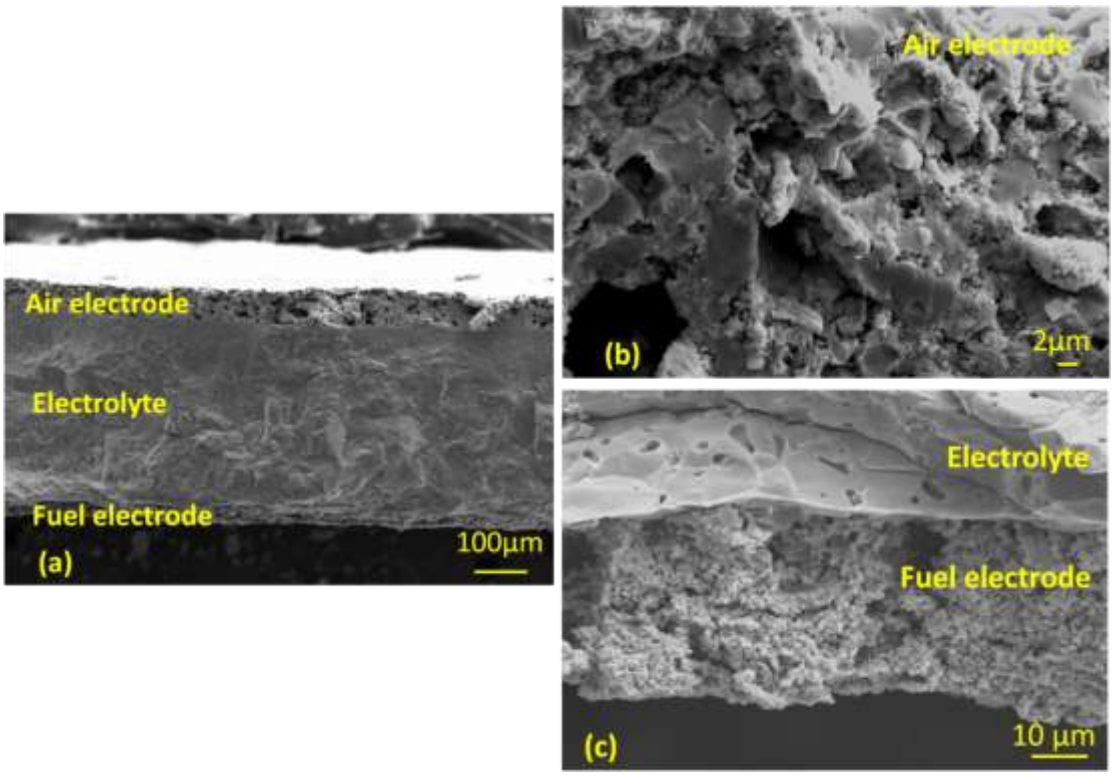


**Fig.S3.** Cross-section view of a post-tested RSOFC (a) whole battery (b) magnified cathode and (c) magnified fuel electrode with electrolyte

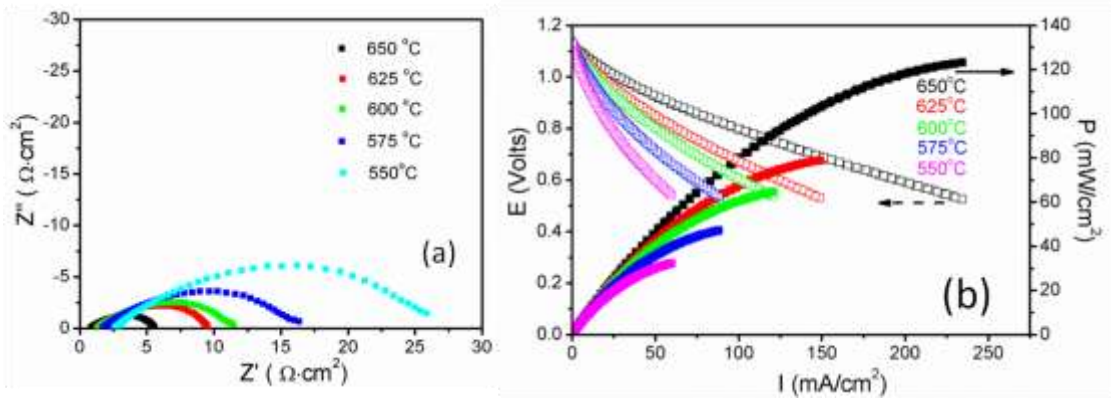


**Fig.S4.** Electrical performance of RSOFC in an open system with a flowing $H_2$+3%$H_2O$ measured from 650°C to 550°C. (a) Impedance spectra; (b) P-I and V-I curves

Fig.S5 shows the morphologies of Mo-based ESM before (a) and after test (b). It is evident that both pre-and post-test redox materials were porous. After test, the porous structures become less uniform with needle-like morphologies appearing in various sizes. The XRD in Fig.S5(c) further confirms that the final product after test consisted of Mo and $MoO_2$, which is consistent with the phase diagram of Mo-O system. [1] The EDX analysis of Fig.S5(d) shows the areas with finer needles are oxygen-rich, which are more likely to be $MoO_2$. The bigger needles may be ascribed to the grain growth

of metallic Mo in 550$^{o}$C during testing.

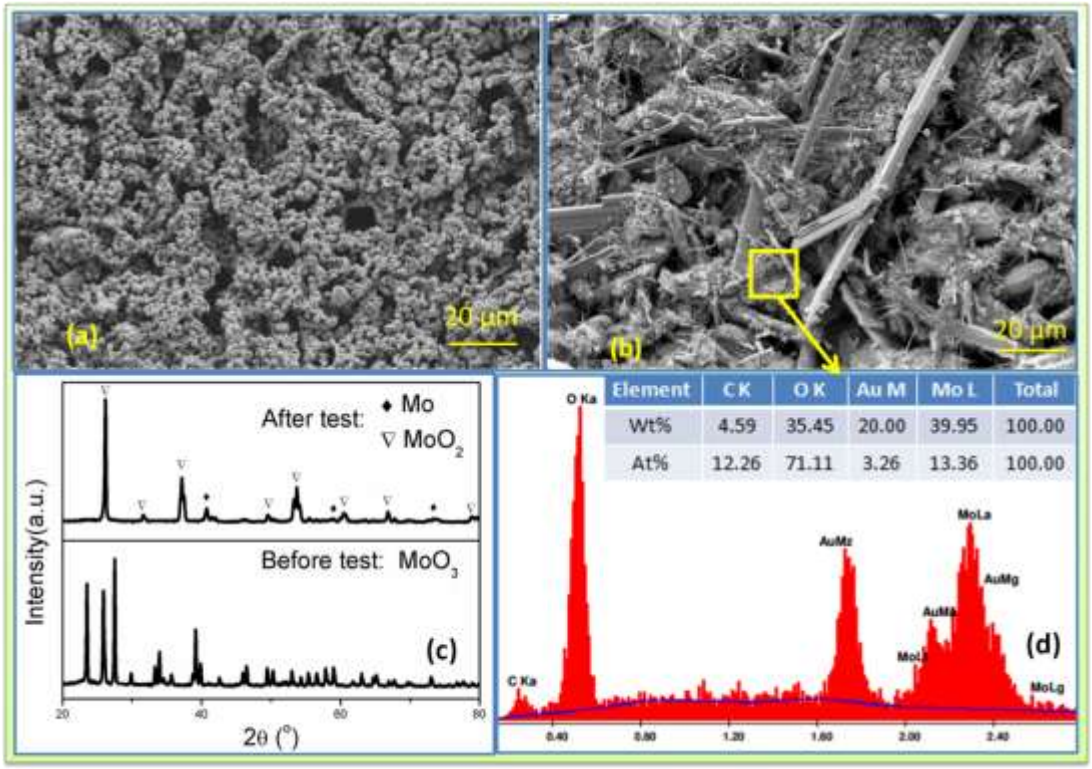


**Fig.S5.** Morphologies of Mo-based ESM (a) pre-test; (b) post-test; (c) XRD-revealed phase evolution before and after test; (d) EDX analysis of post-tested Mo-based ESM

**Reference**

[1] B. Philips, L.L. Y. Chang. *Trans. Metal. Soc*. AIME, **233**, 1433 (1965).
[2] X. Zhao, X. Li, Y. Gong, N. Xu, K. Romito and K. Huang. *Chem. Comm.*, **5357**, 49, (2013).
[3] V. O. Kubaschewski and B. E. Hopkins, Oxidation of Metals and Alloys, New York, 1953.
[4] E. A. Gulbransen and K. F. Andrew. *J. Electrochem. Soc*., **107**, 619,(1960).
[5] E.A. Gulbransen, K. F. Andrew and F.A. Brassart. *J. Electrochem. Soc*., **110**, 952 (1963).
[6] X. Zhao, X. Li, N. Xu and K. Huang, *Solid State Ionics*, **214**, 56 (2012).
[7] Z. Zhan, D. Han, T. Wu, X. Ye, S. Wang, T. Wen, S. Cho and S. A. Barnett, *RSC Adv.*, **2**, 4075 (2012).